

Phonon Hall Effect in Nanoscale Four-Terminal Junctions

Lifa Zhang,¹ Jian-Sheng Wang,² and Baowen Li^{2,3,*}

¹*Department of Physics and Centre for Computational Science and Engineering,
National University of Singapore, Singapore 117542, Republic of Singapore*

²*Department of Physics and Center for Computational Science and Engineering,
National University of Singapore, Singapore 117542, Republic of Singapore*

³*NUS Graduate School for Integrative Sciences and Engineering, Singapore 117597, Republic of Singapore*

(Dated: 9 May 2009)

Using an exact nonequilibrium Green's function formalism, the phonon Hall effect (PHE) for paramagnetic dielectrics is studied in a nanoscale four-terminal device setting. The temperature difference in the transverse direction of the heat current is calculated for two-dimensional models with the magnetic field perpendicular to the plane. We find that there is a PHE in nanoscale paramagnetic dielectrics, the magnitude of which is comparable to the millimeter scale experiments. If the dynamic matrix of the system satisfies mirror reflection symmetry, the PHE disappears. The Hall temperature difference changes sign if the magnetic field is sufficiently large or if the size increases.

PACS numbers: 66.70.-f, 72.15.Gd, 72.20.Pa

In parallel to the study of electronics, phononics gets very active and hot recently[1]. Several conceptual phononic (thermal) devices such as thermal diode, transistor, logic gate and even thermal memory have been proposed to control phonon and process information with phonons. The magnetic field is another degree of freedom could be potentially used to control phonon transport [2]. Indeed, a novel phenomenon – phonon Hall effect (PHE) – has been discovered experimentally by Strohm, et al. [3], which is an analog of the electrical Hall effect for the heat flow in dielectrics. The authors found a temperature difference up to $200\mu\text{K}$ between the sample edges in the direction perpendicular to both the heat flow and the magnetic field. This effect has been confirmed in [4]. The electronic Hall effect is well understood in terms of Lorentz force. However, since no charges are involved and phonons can not couple to the magnetic field directly, it is thus not trial and straight forward to understand the PHE. The magnetic field can polarize the paramagnetic ions; the subsystem of isolated ions carrying magnetic moment M couples to phonons, this spin-phonon interaction (SPI) determines the phonon Hall effect [5, 6].

Theoretical models for PHE have been proposed in Refs. [5, 6], in which phonons are treated ballistically. However, according to Ref.[3], the mean free path ($1\mu\text{m}$) is far less than the system size (15.7 mm), therefore, it is not appropriate to treat the diffusive PHE with ballistic theory. Moreover, in all the previous theoretical work, the spin-phonon interactions were considered by perturbation theory, and they are not consistent with each other.

In this Letter, we would like to address two questions: (1) whether the PHE exists in nano-scale systems, or in other words whether the diffusive PHE can be observed in the ballistic regime; (2) treat the PHE by an exact - non-perturbative theory. The first question is in fact not trivial at all. Since many physics laws valid in macro-

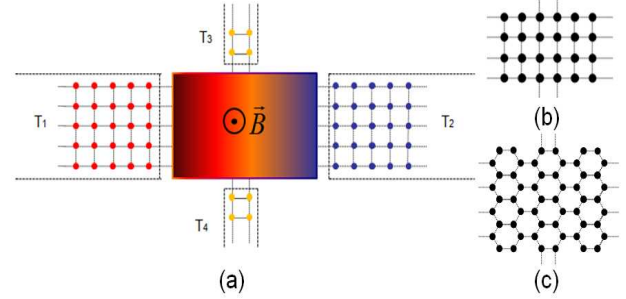


FIG. 1: (color online) The four-terminal PHE setup used for calculating the thermal conductance and the temperature difference $T_3 - T_4$. (a) The left and right leads have temperatures T_1 and T_2 , the upper and lower probe-leads have temperatures T_3 and T_4 . The center part can be different lattices, such as square lattice (b) or honeycomb lattice (c).

scopic scale are not necessary true in nanoscale. For example, Fourier law of heat conduction is broken down in nanoscale[7]. As for the second question, we will take the nonequilibrium Green's function (NEGF) approach. The NEGF is an elegant and powerful method to treat nonequilibrium and interacting systems in a rigorous way. NEGF is widely applied to the electronic and thermal transport, and is successful to study the spin Hall effect in junctions [8].

To develop a nonperturbative theory for PHE in nanoscale four terminal junctions, we consider a model as shown Fig. 1 by taking into account the actual measuring process. The thermal conductance of the system can be calculated by the NEGF method. As we shall see later, our model systems can produce features similar to experiments, even though our systems are of nanometer scale while the experimental systems are of millimeter scale and are in the diffusive regime.

We consider the same Hamiltonian of SPI as in

Refs. [5, 6], which can be expressed in the form $H_I = g \sum_n \vec{s}_n \cdot (\vec{U}_n \times \vec{P}_n)$. Here, \vec{U}_n and \vec{P}_n are the vectors of displacement and momentum of the n -th lattice site. In the presence of a magnetic field \vec{B} , each lattice site has a magnetization \vec{M} . For isotropic SPI, the isospin \vec{s}_n is parallel to \vec{M}_n , and the ensemble average of the isospin is proportional to the magnetization, that is $\langle \vec{s}_n \rangle = c\vec{M}$. Therefore, under the mean-field approximation, the SPI can be represented as

$$H_I = \sum_n \vec{\Lambda} \cdot (\vec{U}_n \times \vec{P}_n), \quad (1)$$

where, $\vec{\Lambda} = gc\vec{M}$, has the units of frequency. According to [5], Λ is estimated to be $0.1 \text{ cm}^{-1} \approx 3 \times 10^9 \text{ Hz}$ at $B = 1 \text{ T}$ and $T = 5.45 \text{ K}$, which is within the possible range of the coupling strength in ionic insulators [9, 10]. In our calculation, we will use this relation to map Λ to magnetic field.

Now we turn to the derivation of the general formula for the temperature difference in the system as illustrated in Fig. 1, where a 2D lattice sample, which can be honeycomb lattice or square lattice, is connected with four ideal semi-infinite leads. We denote the lattice as $N_R \times N_C$, N_R , N_C correspond to the number of rows and columns. We adjust the temperatures of upper and lower probes T_3 and T_4 such that the heat currents from these two leads vanish, namely, $I_3 = I_4 = 0$. Then we get the relative Hall temperature difference as $R = (T_3 - T_4)/(T_1 - T_2)$.

We treat the PHE problem by NEGF method [13] analogous to those used in thermal transport [14]. The total Hamiltonian is assumed to be

$$H = \sum_{\alpha=0}^4 H_{\alpha} + \sum_{\beta=1}^4 U_{\beta}^T V_{\beta,0} U_0 + U_0^T A P_0, \quad (2)$$

where $H_{\alpha} = \frac{1}{2} (P_{\alpha}^T P_{\alpha} + U_{\alpha}^T K_{\alpha} U_{\alpha})$, and A is an antisymmetric, block diagonal matrix with the diagonal elements $\begin{pmatrix} 0 & \Lambda \\ -\Lambda & 0 \end{pmatrix}$. Here, the integers 0 to 4 are associated with the center region, left, right, upper, and lower leads, respectively. U_{α} (P_{α}) are column vectors consisting of all the displacement (momentum) variables in region α . K_{α} is the spring constant matrix and $V_{\beta,0} = (V_{0,\beta})^T$ is the coupling matrix between the β lead and the central region. The dynamic matrix of the full linear system without SPI is

$$K = \begin{pmatrix} K_1 & 0 & V_{1,0} & 0 & 0 \\ 0 & K_3 & V_{3,0} & 0 & 0 \\ V_{0,1} & V_{0,3} & K_0 & V_{0,4} & V_{0,2} \\ 0 & 0 & V_{4,0} & K_4 & 0 \\ 0 & 0 & V_{2,0} & 0 & K_2 \end{pmatrix}. \quad (3)$$

We obtain the equation for U_0 and P_0 as

$$\frac{\partial U_0(\tau)}{\partial \tau} = P_0(\tau) - A U_0(\tau), \quad (4)$$

$$\frac{\partial P_0(\tau)}{\partial \tau} = -K_0 U_0(\tau) - \sum_{\beta=1}^4 V_{0,\beta} U_{\beta}(\tau) - A P_0(\tau). \quad (5)$$

The energy flux to the central region from the lead α is,

$$I_{\alpha} = - \left\langle \dot{H}_{\alpha} \right\rangle = \frac{i}{\hbar} \langle [H_{\alpha}, H] \rangle, \quad \alpha = 1, 2, 3, 4. \quad (6)$$

We define the contour-ordered Green's function as $G^{\alpha\beta}(\tau, \tau') \equiv -\frac{i}{\hbar} \langle T_c U_{\alpha}(\tau) U_{\beta}(\tau')^T \rangle$, where α and β refer to the region that the coordinates belong to and T_c is the contour-ordering operator. Then the equations of motion of the contour ordered Green's function can be derived. In particular, the retarded Green's function for the central region in frequency domain is $G^r[\omega] = \left[(\omega + i\eta)^2 - K_0 - \Sigma^r[\omega] - A^2 + 2i\omega A \right]^{-1}$. Here, $\Sigma^r = \sum_{\alpha=1}^4 \Sigma_{\alpha}^r$, and $\Sigma_{\alpha} = V_{0,\alpha} g_{\alpha} V_{\alpha,0}$ is the self-energy due to interaction with the heat bath, $g_{\alpha}^r = [(\omega + i\eta)^2 - K_{\alpha}]^{-1}$. The lesser Green's function is obtained through $G^< = G^r \Sigma^< G^a$ in the usual way. We thus can calculate the heat flux by the following formula,

$$I_{\alpha} = -\frac{1}{2\pi} \int_{-\infty}^{\infty} d\omega \hbar \omega \text{Re} [\text{Tr} (G^r \Sigma_{\alpha}^< + G^< \Sigma_{\alpha}^a)]. \quad (7)$$

If the temperature differences among the leads are very small, we can regard the system as at linear response regime, $T_{\alpha} = T + \Delta_{\alpha}$. The linearized heat flux from each heat bath can be written as

$$I_{\alpha} = \sum_{\beta=1}^4 \sigma_{\beta\alpha} (\Delta_{\alpha} - \Delta_{\beta}). \quad (8)$$

The conductance from heat bath α to β is defined as

$$\sigma_{\beta\alpha} = \int_0^{\infty} \frac{d\omega}{2\pi} \hbar \omega T_{\beta\alpha}[\omega] \frac{\partial f}{\partial T}, \quad (9)$$

where, $T_{\beta\alpha}[\omega] = \text{Tr}(G^r \Gamma_{\beta} G^a \Gamma_{\alpha})$, $f = (e^{\hbar\omega/k_B T} - 1)^{-1}$, and $\Gamma_{\alpha} = i(\Sigma_{\alpha}^r[\omega] - \Sigma_{\alpha}^a[\omega])$. Therefore, if we set the heat flux of lead 3 and lead 4 to zero, we can get the relative Hall temperature difference as

$$R = (\Delta_3 - \Delta_4)/(\Delta_1 - \Delta_2) = \frac{\sigma_{13}\sigma_{24} - \sigma_{23}\sigma_{14}}{(\sigma_{13} + \sigma_{23} + \sigma_{43})(\sigma_{14} + \sigma_{24} + \sigma_{34}) - \sigma_{43}\sigma_{34}}. \quad (10)$$

Equations (8) and (9) are the Landauer-Büttiker theory [11, 12] applied to the multiple-lead thermal transport.

In the following calculation, We assume a lattice constant $a = 2.465 \text{ \AA}$, and the force constant $K_L = 0.02394 \text{ eV}/(\text{amu} \cdot \text{\AA}^2)$, $K_T = K_L/4$. The ratio of the longitudinal and transverse sound speed to be $\delta = v_L/v_T \approx \sqrt{K_L/K_T} = 2$. Then the speed of sound for longitudinal acoustic phonons is about 4000 m/s . As mentioned above, Λ is estimated to be about $3 \times 10^9 \text{ Hz} \approx 2.0 \times 10^{-6} \text{ eV}$ at $B = 1 \text{ T}$.

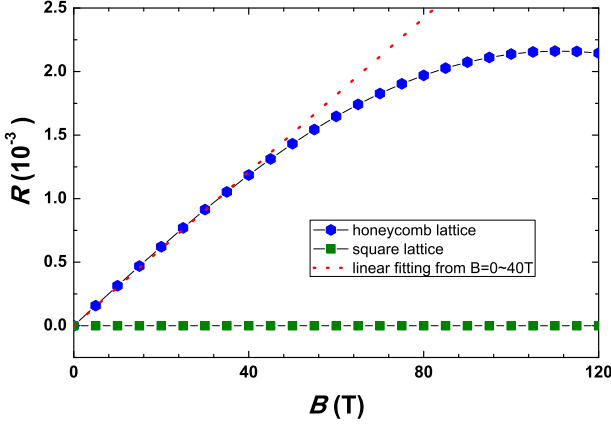


FIG. 2: (color online) Hall temperature difference R versus magnetic field B at temperature $T = 5.45$ K. The hexagon and square line correspond central regions for the honeycomb and square lattices with a nearest-neighbor coupling. The red dotted line corresponds to a linear fit from 0 to 40 T. The size of the center region for honeycomb lattice is 9×6 , the same with the inset (c) in Fig. 1.

From Eq. (10), we find that the relative Hall temperature difference R is an odd function of magnetic field. Onsager relation, $\sigma_{\alpha\beta}(\Lambda) = \sigma_{\beta\alpha}(-\Lambda)$, always holds due to the definition of the conductances. Furthermore, if there is a symmetry operation S such that

$$S K S^{-1} = K, \quad S A S^{-1} = -A, \quad (11)$$

then, $\sigma_{\alpha\beta}(\Lambda) = \sigma_{\alpha\beta}(-\Lambda)$. If this relation is true, then there is no phonon Hall effect in the system. These symmetry considerations are consistent with a different treatment for bulk systems based on Green-Kubo formula [15].

We discuss numerical results in the following. Fig. 2 shows the temperature difference changing with magnetic field at temperature $T = 5.45$ K for the honeycomb and square lattices with nearest-neighbor couplings. For the honeycomb case, the Hall temperature is odd and linear in the magnetic field between 0 and 40 T, in that range the slope of the curve is 3×10^{-5} K/T, comparable to the experimental data in Ref. [3]. When the magnetic field is extremely large, it will decrease. From our calculation, we find that the triangular lattice has a similar behavior. However, for square lattice with the nearest-neighbor coupling, there is no PHE at all. The spring constant matrix between every nearest coupling sites is diagonal for the square lattice. This matrix and also the full matrix K is invariant with respect to a reflection in x or y direction, thus satisfying Eq. (11). If we consider next-neighbor couplings of the lattice, the dynamic matrix K will not have the mirror reflection symmetry, and the PHE can come out.

We show the conductances among different leads in Fig. 3. We set all the couplings between the leads and central region the same, and all the leads and central

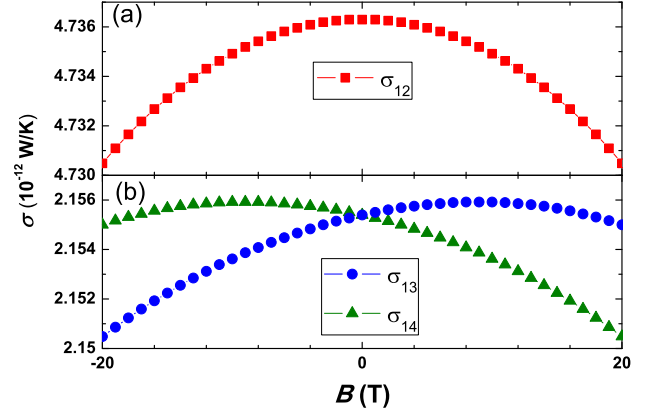


FIG. 3: (color online) Thermal conductance versus the magnetic field at temperature $T = 5.45$ K for the honeycomb lattice. (a) shows the conductance between two longitudinal leads σ_{12} . (b) shows the conductance between one longitudinal lead and one transverse probe-lead. The circle and triangular lines correspond to σ_{13} and σ_{14} , respectively. The size of center region is 9×6 .

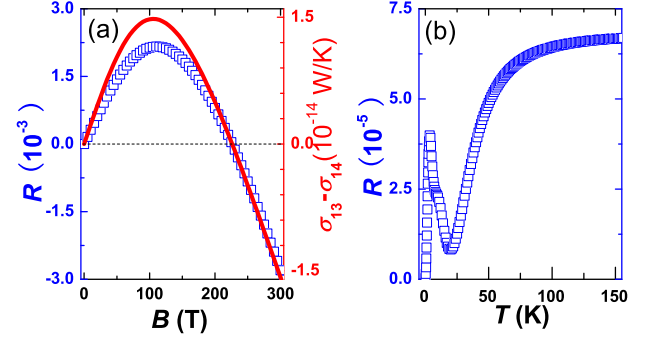


FIG. 4: (color online) The relative Hall temperature difference R versus the large magnetic field B (a) and high equilibrium temperature T for honeycomb lattice (b). (a) square shows R changing with the magnetic field (left scale), the red solid line shows the conductance difference $\sigma_{13} - \sigma_{14}$ versus magnetic field (right scale). (b), R vs. equilibrium temperature at $B = 1$ T.

region have the same spring constants for simplicity. Because of the symmetry of the system, we have additional relations, $\sigma_{13} = \sigma_{32} = \sigma_{24} = \sigma_{41}$, and $\sigma_{14} = \sigma_{42} = \sigma_{23} = \sigma_{31}$. We find that the conductance between two longitudinal leads or two transverse probe-leads are even in the magnetic field, which can be seen in Fig. 3(a), σ_{34} has the same property. However, for honeycomb lattice the conductance between one longitudinal lead and one transverse probe-lead is not an even function of magnetic field [Fig. 3(b)], which gives contribution to the Hall temperature difference. Therefore, for honeycomb lattice, the temperature difference is not zero. But for square lattice, σ_{13} is an even function of magnetic field, the same is true for other components. no PHE exists in such systems.

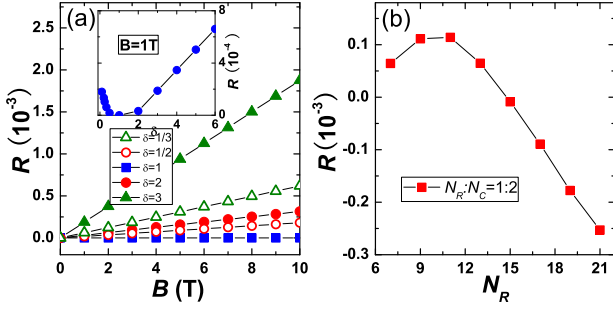


FIG. 5: (color online) (a) The relative Hall temperature difference versus magnetic field for different ratio of the longitudinal and transverse sound speed $\delta = v_L/v_T$. The inset shows R versus δ at $B = 1$ T. The data are calculated for 9×6 honeycomb lattice at $T = 5.45$ K. (b) The relative Hall temperature difference versus the number of rows of atoms for fixed aspect ratio $N_R : N_C = 1 : 2$ at $B = 1$ T and $T = 5.45$ K.

We show the numerical results for the ratio R at $T = 5.45$ K for honeycomb lattice in Fig. 4(a). The temperature difference will not be linear when the magnetic field is larger than 40 T, after about 110 T, it will decrease, and about $B_c \approx 230$ T, R changes sign to negative. It is the same critical point for the difference of conductances $\sigma_{13} - \sigma_{14}$, which is consistent with Eq. (10). In Fig. 4(b), we show R versus temperature at $B = 1$ T. When the temperature increases, R will increase almost linearly. After some value, it decreases, and then increases again. At last, it tends to a constant. This behavior is due to the competition of the numerator and denominator in Eq. (10). When temperature is very high, all the conductances tend to constants due to ballistic thermal transport.

In Ref. [5], it is reported that R decreases with increasing ratio of the longitudinal and transverse sound speed $\delta = v_L/v_T$ and changes sign when δ becomes large than 5. However, we find that when the ratio ($\delta > 1$) become large, R increases, see Fig. 5(a). At exactly $\delta = 1$, when the longitudinal speed equals to the transverse speed, there is no PHE, which testifies our condition, Eq. (11), for the absence of PHE. All the spring constant matrices between the nearest-neighbors become diagonal at $\delta = 1$, the condition Eq. (11) holds for a mirror reflection operation. If $\delta < 1$, R increases again with the decreasing of δ . Although the ratio R does not change sign with δ , due to the ballistic nature of a small system, the ratio R is sensitive to the geometric details, which is shown in Fig. 5(b), the magnitude and the sign of R will change with the size increasing.

In conclusion, a theory for PHE in nanoscale paramagnetic dielectrics by NEGF approach is developed. The results are consistent with the essential experimental features of PHE, such as the magnitude and linear magnetic field dependence of the observed transverse temperature

difference. We find that there is no PHE if the lattice satisfies a certain symmetry. The symmetry of the dynamic matrix K is the key point for the existence of PHE. The Hall temperature difference changes with equilibrium temperature and tends to be a constant at last. And the Hall temperature difference does not change sign with the ratio of the longitudinal and transverse sound speed in the range of $\delta \in (0.1, 10)$.

Most of our results should be verified by experiments on nano-scale paramagnetic dielectrics, which can have potential applications to controlling nanoscale phonon transport. For most paramagnetic dielectric materials, because of the complexity of the coupling (such as next or next-next neighboring interaction), the dynamic matrix does not satisfy the mirror reflection symmetry, the PHE can be present. The Hall temperature difference behavior with magnetic field can be measured in a strong magnetic field (if $\Lambda = 2.0 \times 10^{-5}$ eV, the magnetic field will be ten times smaller). From our study, the PHE can be measured in nanoscale system at relative high temperature (~ 100 K).

We thank Jinwu Jiang, Yonghong Yan, Jie Chen and Jie Ren for fruitful discussions. L. Z. and B. L. are supported by the grant R-144-000-203-112 from Ministry of Education of Republic of Singapore. J.-S. W. acknowledges support from a faculty research grant R-144-000-173-112/101 of NUS.

* Electronic address: phylibw@nus.edu.sg

- [1] L. Wang and B. Li, Physics World **21**, No.3, 27 (2008).
- [2] L. Zhang, J.-S. Wang and B. Li, Phys. Rev. B **78**, 144416 (2008); Y.-H. Yan, C.-Q. Wu and B. Li, Phys. Rev. B **79**, 014207 (2009).
- [3] C. Strohm, G. L. J. A. Rikken, and P. Wyder, Phys. Rev. Lett. **95**, 155901 (2005).
- [4] A. V. Inyushkin and A. N. Taldenkov, JETP Lett. **86**, 379 (2007).
- [5] L. Sheng, D. N. Sheng, and C. S. Ting, Phys. Rev. Lett. **96**, 155901 (2006).
- [6] Yu. Kagan and L. A. Maksimov, Phys. Rev. Lett. **100**, 145902 (2008).
- [7] C.-W. Chang et al, Phys. Rev. Lett. **101**, 075903 (2008).
- [8] L. Sheng, D. N. Sheng, and C. S. Ting, Phys. Rev. Lett. **94**, 016602 (2005).
- [9] R. Orbach, Proc. R. Soc. A **264**, 458 (1961).
- [10] *Spin-Lattice Relaxation in Ionic Solids*, edited by A. A. Manenkov and R. Orbach (Harper & Row, New York, 1966).
- [11] S. Datta, *Electronic Transport in Mesoscopic Systems* (Cambridge Univ. Press, 1995).
- [12] M. Büttiker, Phys. Rev. Lett. **57**, 1761 (1986); M. Büttiker, IBM J. Res. Developm. **32**, 317 (1988).
- [13] H. Haug and A. P. Jauho, *Quantum Kinetics in Transport and Optics of Semiconductors* (Springer, 1996).
- [14] J.-S. Wang, J. Wang, and N. Zeng, Phys. Rev. B **74**, 033408 (2006); J.-S. Wang, J. Wang, and J. T. Lü, Eur. Phys. J. B **62**, 381 (2008).

- [15] J.-S. Wang and L. Zhang, arXiv:0902.1219v1.